Journal of Electrocardiology 86 (2024) 153762

Contents lists available at ScienceDirect

Journal of Electrocardiology

journal homepage: www.jecgonline.com

Simulating left atrial arrhythmias with an interactive N-body model

Bryant Wyatt [a,*], Gavin McIntosh [a], Avery Campbell [b], Melanie Little [c], Leah Rogers [a], Brandon Wyatt [d]

[a] Tarleton State University, Department of Mathematics,1333 W Washington St, Stephenville, TX 76401, United States of America
[b] Oncor Electric Delivery, 1616 Woodall Rodgers Fwy, Dallas, TX 75202, United States of America
[c] MD Anderson School of Health Professions, 1515 Holocombe Blvd, Houston, TX 77030, United States of America
[d] Biosense Webster, 31 Technology Dr. Suite 200, Irvine, CA 92618, United States of America

ARTICLE INFO

Keywords:
Supraventricular tachycardia
Computer modeling
Electrophysiology
Catheter ablation
Left atrium
Heart arrhythmias

ABSTRACT

Background: Heart disease and strokes are leading global killers. While atrial arrhythmias are not deadly by themselves, they can disrupt blood flow in the heart, causing blood clots. These clots can travel to the brain, causing strokes, or to the coronary arteries, causing heart attacks. Additionally, prolonged periods of elevated heart rates can lead to structural and functional changes in the heart, ultimately leading to heart failure if untreated. The left atrium, with its more complex topology, is the primary site for complex arrhythmias. Much remains unknown about the causes of these arrhythmias, and computer modeling is employed to study them.
Methods: We use N-body modeling techniques and parallel computing to build an interactive model of the left atrium. Through user input, individual muscle attributes can be adjusted, and ectopic events can be placed to induce arrhythmias in the model. Users can test ablation scenarios to determine the most effective way to eliminate these arrhythmias.
Results: We set up muscle conditions that either spontaneously generate common arrhythmias or, with a properly timed and located ectopic event, induce an arrhythmia. These arrhythmias were successfully eliminated with simulated ablation.
Conclusions: We believe the model could be useful to doctors, researchers, and medical students studying left atrial arrhythmias.

Introduction

Heart disease and strokes are the leading causes of death worldwide [1,2]. Supraventricular Tachycardia (SVT) is a significant contributing factor to strokes, heart failure, and, in some cases, acute myocardial infarction [3–5]. Therefore, it is imperative that in our pursuit of building healthier lives free of cardiovascular diseases and strokes, we focus on reducing the occurrence of SVT.

SVT encompasses all cardiac arrhythmias where the underlying mechanism sustaining the abnormal heartbeat originates above the ventricles. This abnormal heartbeat can disrupt the natural synchronization between the atria and the ventricles, disturbing the laminar blood flow through the heart and causing it to stagnate in the small finger-like appendage of the left atrium (LA). Consequently, this allows for the formation of certain types of lethal blood clots known as mural thrombi, which can become dislodged and travel to the brain or coronary arteries, resulting in a stroke or heart attack [6]. This mechanism leads individuals with atrial fibrillation (AF) to experience a five-fold increased risk of stroke [7]. In addition to the blood stagnation caused by the chaotic action of AF, prolonged periods of elevated heart rates from simple periodic tachycardias can lead to structural and functional changes in the heart muscle known as tachycardia-mediated cardiomyopathy (TMC), ultimately causing heart failure if left untreated [8].

In a normally functioning heart, the sinus node serves as the pacemaker, consistently producing an electrical impulse to dictate the heart's rhythm and rate. This electrical impulse initiates a chain reaction that propagates throughout the heart, generating a life-sustaining heartbeat. Ectopic electrical impulses can lead to chain reactions occurring at the wrong place and time, disrupting the normal sinus rhythm. This disruption may cause the atria to flutter, beat out of sync with the ventricles, or present a myriad of other undesirable outcomes [9].

In many cases, SVT can be successfully controlled with medication and lifestyle changes. However, some of these drugs are challenging for

* Corresponding author.
E-mail address: wyatt@tarleton.edu (B. Wyatt).

https://doi.org/10.1016/j.jelectrocard.2024.153762

Available online 22 July 2024

patients to tolerate, and certain medications with the most established efficacy are known to be hepatotoxic, causing deleterious side effects [10]. Hence, catheter ablation, though more invasive than medication therapy, has proven to be the most reliably efficacious and safest method physicians have for treating patients with recurring SVT [11–14].

Radiofrequency (RF) catheter ablation and three-dimensional electro-anatomical mapping techniques have seen dramatic improvement over the last 10 years, enabling doctors to perform procedures on beating hearts that were, until recently, thought impossible [15,16]. However, much is still not understood about what causes heart arrhythmias and how to use RF catheter ablation to treat them [17]. What would assist doctors, researchers, and medical students is a way to rapidly and inexpensively test ideas and observe outcomes. We have created an N-body computer model of the LA to do just this.

The LA was chosen because it is the site where most complex arrhythmias arise [18–21]. The model captures both electrical and mechanical activity. Users can adjust the model down to the individual muscle level and introduce ectopic events. Note: In this text when we refer to a muscle, we mean a group of cardiomyocytes. These tools can be used to induce arrhythmias in the LA that can be eliminated through simulated ablations. All of these actions can be performed interactively in a running simulation, enabling users to set up conditions in the simulated LA, test ablation strategies, and observe the outcomes.

Methods

Model selection

Tissue is composed of a system of cells that interact with each other mechanically, chemically, and electrically. When modeling a significant amount of tissue, the sheer number of cells that need to be simulated computationally at the cellular level becomes too large. Hence, one is faced with two choices:

1. Represent the tissue as a single continuum and model the entire system with a comprehensive set of equations [22–25]. This type of modeling, in general, is less computationally expensive but may lack the necessary complexity to capture variant behaviors such as atrial arrhythmias [26].
2. Define discrete units (sometimes referred to as agents or automata) that can represent groups of cells. Then, establish a corresponding set of rules or functions that each unit follows [27–31]. This type of modeling, in general, is more computationally intensive but enables the creation of more complex systems capable of capturing intricate cardiac events.

In this work, we chose to use the second type of model due to the flexibility it offers in adjusting the rules at the individual unit level. For models where only electrical and/or chemical interactions are of interest, Cellular Automaton models are typically used [32]. Cellular Automaton models were made popular in the 1970s by John Conway's "Game of Life" [33]. The simple rules laid out by Conway in the "Game of Life" can lead to the spontaneous emergence of recurrent patterns, similar to those observed in atrial arrhythmias.

However, because we were interested not only in electrical and chemical processes but also in mechanical processes, we chose an N-body model. In an N-body model, the agents are allowed to move, which enabled us to incorporate pressure into the model and potentially add blood flow in the future.

N-body problems and the Leapfrog formulas

N-body models are in the class of models known as agent-based models, which encapsulate all of the discrete (second type) models described above [34,35]. Historically N-body models were used to model the motion of planets in our solar system. In this approach, each planet is treated as a point mass, and the planets interact through the force of gravity [36,37]. In astrophysics, large aggregates of point mass units/bodies can be used to study phenomena such as planet formations [38,39]. This concept can be extended from studying large-scale events to extremely small-scale events, as seen in chemistry, where it is commonly referred to as molecular dynamics or quasi-molecular modeling [40,41]. In this context, each molecule or atom is treated as a point mass and point charge; these units/bodies typically interact through electrical forces. In mechanical engineering, lattice structures can be simplified by reducing connecting rods to point mass units/bodies that interact through Hookean forces [42]. Once a force system is determined, the movement of the bodies is governed by Newton's laws of motion. While many numerical methods exist to integrate N-body problems forward in time, the Leapfrog formulas were chosen for this project due to their combination of accuracy and simplicity [43,44].

Cardiac tissue simulation

Cardiac tissue is modeled as a network of nodes and connectors. The nodes carry the mass and spatial attributes of the tissue. The connectors control the force between nodes and transport the electrical signal throughout the tissue. The nodes are point masses, and the connectors are massless Hookean springs that also serve as timed signal transports. Each node is a standalone unit, keeping track of its mass, spatial location, attached connectors, and whether it is on or off (ablated). Connectors are also standalone units, with each unit keeping track of its resting length, rest strength, contraction length, contraction strength, contraction duration, recharge duration, conduction velocity of its electrical signal, and signal direction. Each connector also contains an internal clock to keep track of its internal processes.

In short, the grid of nodes and connectors acts as a Cellular Automaton system that transports electrochemical processes through the LA over time. Additionally, the grid of nodes and connectors functions as a semi-connected N-body system that changes the shape of the LA over time.

The mass of each node and the contractile strength of each connector depend on the total mass of the simulated tissue. To achieve this, we distribute the mass of the tissue across all connectors. It's important to note that this distribution is only done to set node masses and connector strengths, as connectors themselves are considered massless. The mass assigned to a connector is calculated by multiplying the total tissue mass by the length of the connector and then dividing the result by the total lengths of all connectors.

The mass of a node is determined by half of the combined mass of its attached connectors (Eq. (1)). This multiplication by one-half is applied because each connector contributes one-half of its mass to each of the two nodes it connects.

The contractile force of each connector is calculated by multiplying its mass by the force-per-mass ratio of a myocyte (Eq. (2)). This ratio is crucial for collaborating a connector's force relative to that of a myocyte. The resting strength of a connector is utilized to restore the tissue to its original shape. This attribute plays a significant role in maintaining the shape of the simulated tissue.

$$Mass\ of\ node_i = \frac{TM}{2^{*}TCL}\sum_j CL_j \tag{1}$$

$$Contractile\ strength\ of\ connector_i = SR^{*}CM_i \tag{2}$$

here, TM equals the total mass of the tissue, TCL equals the total length of all connectors in the system, CL_j is the length of the j^{th} connector, and j runs through all connectors joined to the i^{th} node. SR is the force per mass ratio of a myocyte and CM_i is the mass of the i^{th} connector (Table 1).

The connectors (referred to as muscles for the remainder of this text) produce the contractile force of the tissue and transition between two

Table 1
Typical parameter run values.

	Values
Myocyte Force/Mass Ratio	596.00 mm/ms^2
Rough Estimated Mass of Left Atrium	25.00 g
Rough Estimated Radius of Left Atrium	17.8 mm
Muscle Compression Stop Fraction	0.70
Beat Period	1000.00 ms
Base Muscle Contraction Duration	200.00 ms
Base Muscle Recharge Duration	200.00 ms
Base Conduction Velocity	0.50 mm/ms

We will refer to the refractory period as the sum of the contraction duration and the recharge duration.

states: the resting state and the contracting state. This transition is achieved by simply changing the muscle's natural length and spring constant. The difference between the resting and contractile lengths is set by the Muscle Compression Stop Fraction (Table 1).

To create a beat, one node is selected as the pulse node and stimulated with a periodic signal. This pulse node is drawn larger in the simulation and is green when the simulation is running and red when the simulation is paused. When stimulated, the pulse node will try to activate all of the muscles connected to it. If a muscle is already contracting or in its recharge state, it will ignore the stimulus. However, if the muscle is rested and ready to contract, it will transition into its contraction state, reset its internal clock, and start a signal propagation down its length away from the stimulating node. When this signal reaches the end of the muscle, it will stimulate the other node it is connected to. If this node is ablated, it will ignore the signal. However, if the node is alive, it will try to activate all the muscles it is connected to. This creates a chain reaction down the tissue and a beat will emerge.

Callback functions and user simulation interaction

Callback functions allow hardware and software to interact and are used here so that users can adjust node and muscle attributes in an active simulation [45]. Initially, all node and muscle attributes are read from a user-defined setup file. Once a simulation is running, mouse and keyboard callback functions allow the user to adjust node and muscle settings either in groups or individually at any time during an active simulation.

The user can ablate nodes, change the duration of muscle contraction and recharge periods, and adjust the propagation speed of a muscle's electrical signal. Additionally, the user can place an ectopic event anywhere and at any time in a running simulation. This is accomplished by moving the mouse over a node and stimulating it with a left click, starting a single chain reaction at that node. Furthermore, the user can place an ectopic beat in a similar manner. For an ectopic beat, the user will be asked for a pulse frequency, and the ectopic node will act like the pulse node, competing for control of the beat.

The difference between an ectopic event and an ectopic beat is that an ectopic event is a one-time ectopic trigger, whereas an ectopic beat is a recurrent periodic ectopic trigger. Callback functions also allow the user to change views, take snapshots, make videos, and store model settings for later use.

We believe that the interaction between the user and the simulation is what makes this model novel. Electrophysiologists and researchers can set up specific scenarios, observe the outcomes, and then experiment with ablation schemes to study the resulting effects. Medical students could be tasked with creating arrhythmias in the model, which would provide them with a deep understanding of the causes of that type of arrhythmia.

Overview of simulation coloring schemes

The pulse node, as stated earlier, is green when the simulation is running and red when the simulation is paused. Other nodes are green when they are active and white when they are ablated. You can ablate the pulse node, which will terminate its periodic signal and cause it to turn white. If you create an ectopic beat, the selected node will turn purple, allowing the user to see where the rogue beat is originating from. An ectopic event, which is just an isolated single rogue signal, will not change the colour of the node.

Muscles will be red when they are ready to contract, yellow when they are contracting, and pink when they are recharging. If the user changes the attributes of a group of muscles, the simulation will pause, the nodes associated with the adjusted muscles will turn blue, and the muscles that have been adjusted will turn purple. When the simulation is continued, the muscles will return to their red, yellow, and pink cycle, but the nodes associated with the adjusted muscles will remain blue to allow the user to keep track of the regions that were adjusted.

If node viewing is turned off, which speeds up simulations and is useful in simulations with higher node counts, the pixels in the regions of white (ablated) nodes, blue (adjusted) nodes, and purple (ectopic beat) nodes will be colored white, blue, and purple, respectively. The green nodes, which will make up the majority of nodes, will simply not be seen.

One-dimensional model

We began work on a one-dimensional model to demonstrate that an electrical wavefront periodically stimulated from a single node (the pulse node) would propagate down a strand of cardiac muscles and initiate a chain reaction of contractions (a beat). We tested the model to see if the electrical wavefront would terminate at ablated nodes. Additionally, nodes were excited with ectopic events in front of the electrical wavefront to observe if a competing wavefront would propagate from this location and interrupt the original wavefront. A graphical user interface was also developed using OpenGL (Fig. 1 and Video 1).

Two-dimensional model

Building on the insights obtained from the one-dimensional model, we created a two-dimensional model. To construct this model, we connected the end of the muscle chain back to the pulse node (Fig. 2). This arrangement enabled us to test the propagation of electrical wavefronts in two directions and observe how they terminated upon encountering each other (Video 2). The introduction of this extra dimension also allowed us to create a slow and fast pathway. Using the ablation feature of the model to block and release, we were able to create a textbook reentry tachycardia that seized control of the beat from the pulse node (Video 3).

Three-dimensional model

The transition to three dimensions enabled us to test the propagation of electrical wavefronts in multiple directions and observe their termination on muscles that were in their refractory period or on nodes that had been ablated. We also verified whether the model could produce a realistic beat (Fig. 3 and Video 4). Additionally, we removed the top and bottom nodes and placed the pulse node on the edge of the top hole. This was done to create a crude representation of the right atrium, where the top hole represented the superior vena cava, the bottom hole represented the inferior vena cava, and the pulse node represented the sinus node. Blood pressure was simulated with an outward central force applied to each node. In the future, we plan to replace this force by filling the cavity with simulated blood. Our end goal was to model the LA, but at this point in the development, the right atrium provided the model with some structural validity. In three dimensions, we were able to slow the conduction velocity in a small group of muscles and produce a micro-reentry tachycardia (Video 5).

With a functional three-dimensional model in place, we were ready

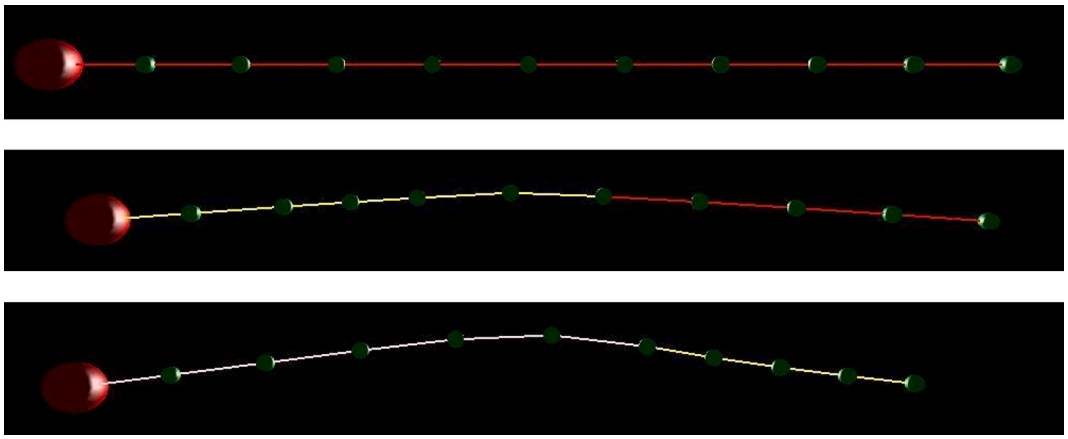

Fig. 1. Screenshots represent the simulated cardiac muscle tissue going through a beat cycle (images should be read from top to bottom). The large red sphere represents the pulse node. The smaller green spheres represent the other nodes. The lines connecting the nodes are muscles. When a muscle is ready to contract, it is red; when contracting, it is yellow; and when recharging, it is pink. Refer to Video 1 for a demonstration of a beat cycle, as well as a demonstration of the ectopic event and ablation tools. (For interpretation of the references to colour in this figure legend, the reader is referred to the web version of this article.)

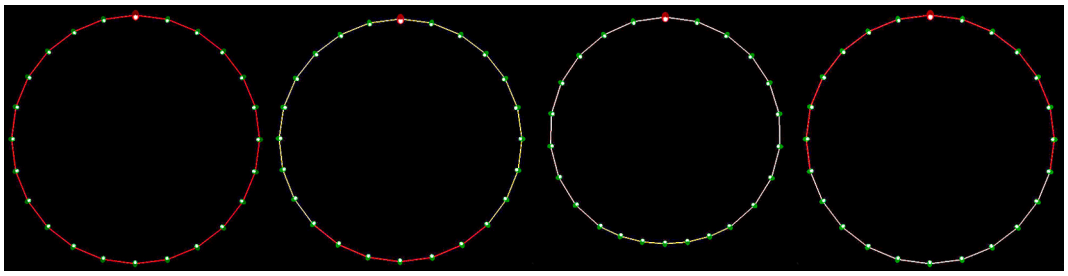

Fig. 2. Screenshots representing a two-dimensional ring of myocardium completing a beat (images should be read from left to right). Red indicates readiness to contract, yellow indicates contraction, and pink indicates recharging (Video 2). Refer to Video 3 for a demonstration of a simple reentry tachycardia seizing control of the beat. (For interpretation of the references to colour in this figure legend, the reader is referred to the web version of this article.)

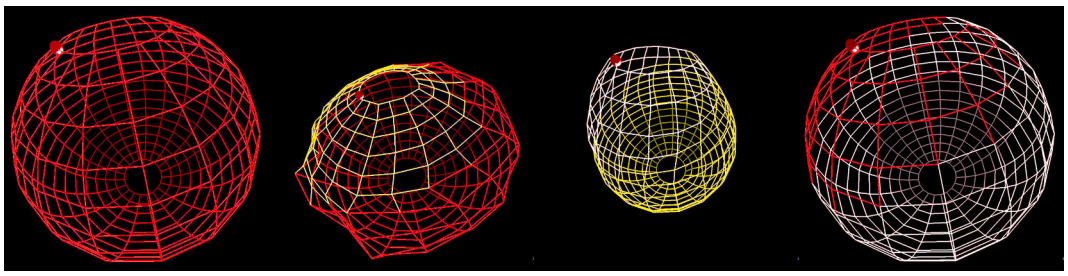

Fig. 3. Screenshots representing a three-dimensional sphere of myocardium completing a beat (images should be read from left to right). Red indicates readiness to contract, yellow indicates contraction, and pink indicates recharging. The visualization of the individual nodes has been removed because this many spheres clutter the image. The pulse node is still represented here as a red sphere (Video 4). See Video 5 for a demonstration of a micro-reentry tachycardia. (For interpretation of the references to colour in this figure legend, the reader is referred to the web version of this article.)

to increase both the node and muscle count. However, this resulted in a higher computational demand on the limited number of central processing unit (CPU) cores, causing the simulations to run too slowly for an interactive environment. Consequently, we rewrote the code, implementing parallel processing and distributing the workload across the thousands of cores on a graphics processing unit (GPU).

In Fig. 4 and Video 6, we demonstrate a micro-reentrant tachycardia created by reducing the refractory period and conduction velocity (short wavelength) in a group of muscles [46]. Subsequently, we isolated this reentry through simulated ablations, restoring the atrium to sinus rhythm. The video shows that it can take several attempts to completely isolate the rogue tissue.

Results

Idealized left atrium

With a functional three-dimensional model designed to run on parallel hardware and optimized for NVIDIA GPUs, we proceeded to create an idealized representation of the LA. Utilizing Blender, an open-source three-dimensional rendering software package, we crafted an anatomically accurate structure of the LA, incorporating the four pulmonary vein openings and the mitral valve in their correct positions. The pulse node was strategically placed where Bachmann's bundle enters the LA. Although we did not simulate the branches of Bachmann's bundle in this version, it is planned for inclusion in a later iteration of the model.

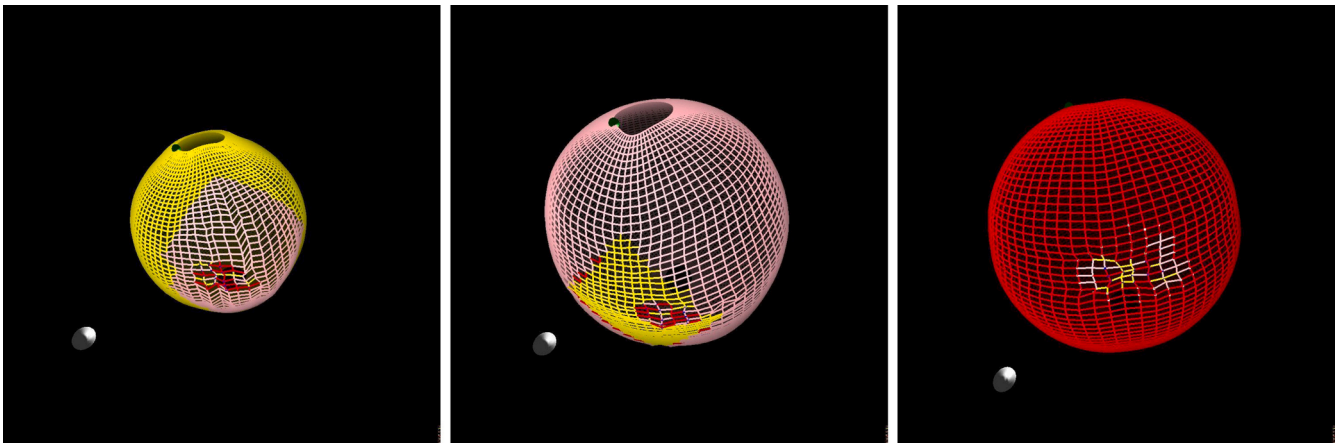

Fig. 4. Screenshots depict a micro-reentry and its isolation on the refined model with increased node and muscle count. The first two images show the reentry in control of the beat. The third image shows the isolated reentry, restoring the atrium to sinus rhythm (Video 6).

Additionally, a more complex muscle structure was implemented, and the appendage was removed to enhance the model's usability (Fig. 5 and Video 7).

Left atrial arrhythmias

With a model of the LA in place, our objective was to demonstrate the reproduction of common LA arrhythmias by adjusting muscle characteristics in specific areas of the LA. Subsequently, we aimed to simulate the removal of these arrhythmias through ablations, all within an active simulation.

Initially, we created a micro-reentry by reducing the refractory period and conduction velocity in a section of muscle tissue. This resulted in a micro-reentry taking control of the beat. Through ablation around the micro-reentry, we were able to isolate it from the rest of the atrium and restore the atrium to sinus rhythm (Fig. 6 and Video 8).

Next, we induced a LA flutter by slowing the conduction velocity of the muscles between two pulmonary vein openings and introducing an ectopic trigger at just the right location and time. The ectopic trigger generated a flutter around the LA, seizing control of the beat. By ablating between these two pulmonary vein openings, we eliminated the flutter (Fig. 6 and Video 9).

In the third scenario, we created a LA with isolated pulmonary veins and a faulty ablation joining the pulmonary vein groupings. The adjoining ablation had regrown tissue that was damaged, causing slow conduction (muscles connecting blue nodes). With a properly timed ectopic event at the fault, we induced an LA flutter. Subsequently, we removed the flutter by repairing the fault (Fig. 6 and Video 10). Note: In this video, some muscles connecting ablated nodes were adjusted. These muscles will remain purple because they can not be stimulated, allowing them to return to their red, yellow, and pink cycle.

Patient-specific models

The gold standard for any medical modeling software is to be patient-specific. We acquired open-source spatial data of a real LA [47]. Using Blender, we removed the appendage and performed slight data cleaning. The resulting spatial data was then fed into the model. For context, in this model, the average muscle length is approximately one millimeter. Applying our standard electrical setup, the simulation ran remarkably well. We were able to ablate sections of the atrium. Additionally, by reducing the refractory period and conduction velocity in a portion of muscle tissue, we successfully created a micro-reentry (Fig. 7 and Video 11). Note: In Video 11, the ablated region and the micro-reentry are not related in any way; they are just demonstrated in a single simulation. We believe that it should be possible to take spatial data from CT scans and create a useful model of a patient's heart, enabling physicians to perform test procedures.

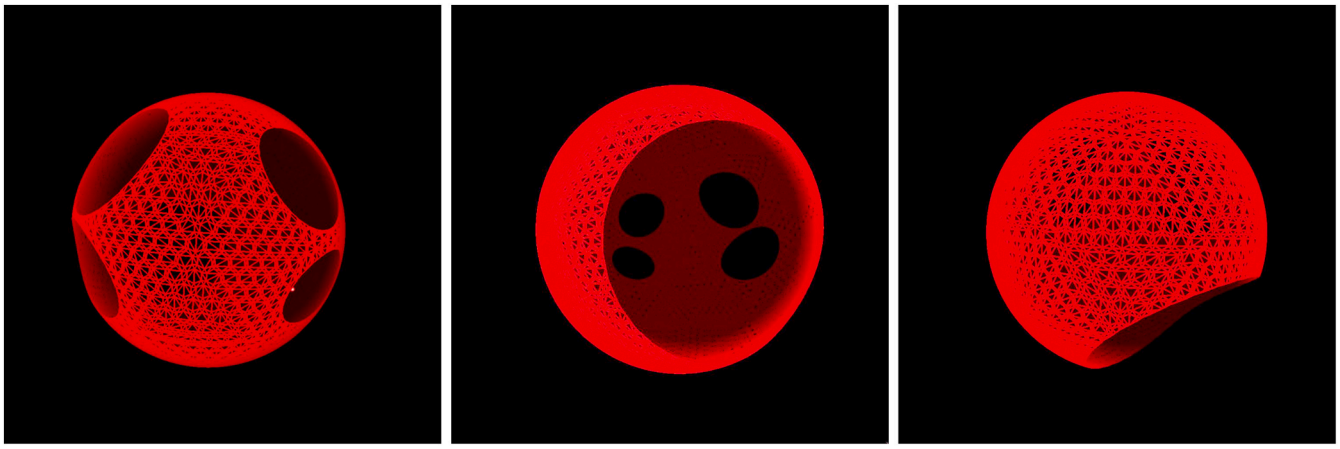

Fig. 5. Images of the idealized LA: The first image depicts a view from the back, showcasing the four pulmonary vein openings. The second image provides a perspective through the mitral valve, looking up and back toward the four pulmonary vein openings. The third image offers a frontal view, highlighting the mitral valve. Refer to Video 7 for an overview of the idealized LA model going through a beat cycle.

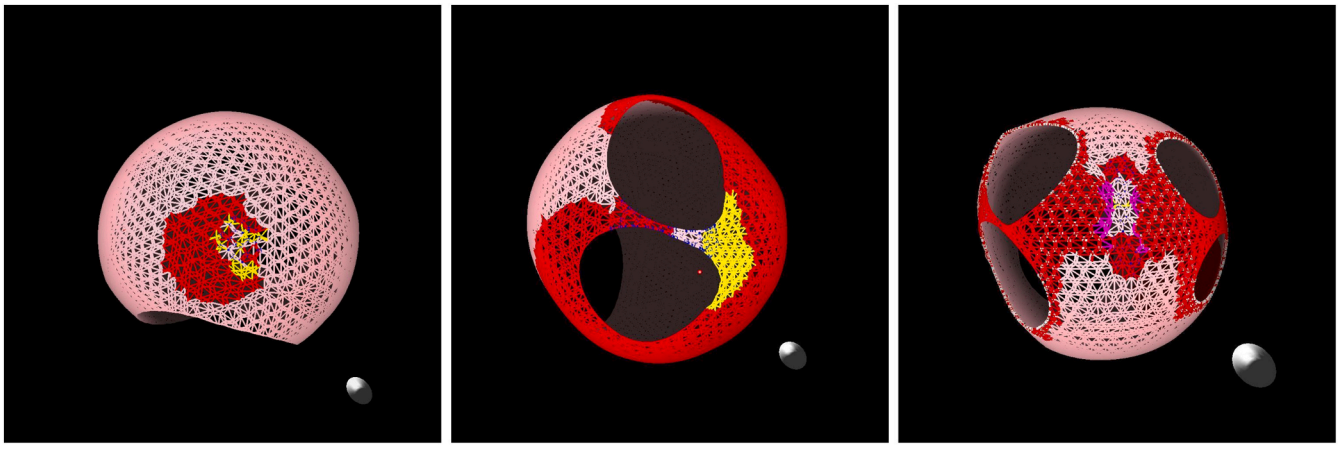

Fig. 6. Images of the idealized LA in common arrhythmias: The first image shows a micro-reentry on the LA (Video 8). The second image displays a LA flutter between two pulmonary vein openings caused by slow conduction velocity between the openings and an ectopic event (Video 9). The third image illustrates a LA that has undergone pulmonary vein isolation and an ablation joining the pulmonary vein groupings. The adjoining ablation has an electrical leak with slowed conduction through the leak. This situation does not cause a problem until an ectopic event triggers a flutter (Video 10).

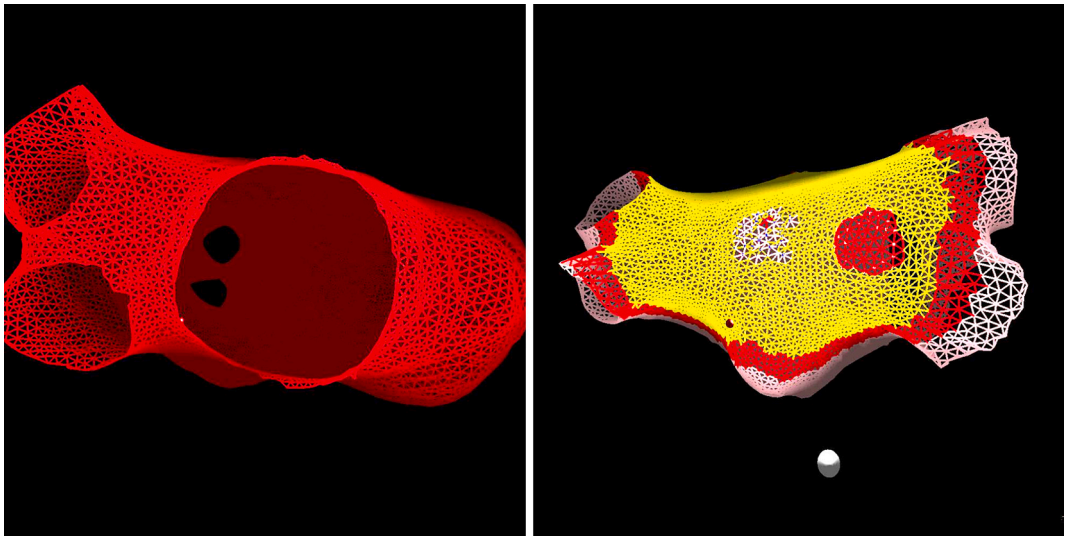

Fig. 7. Images of a real LA: The first image provides a view of the LA showing the mitral valve and the four pulmonary vein openings. The second image offers a frontal view, highlighting a section of the atrium where a micro-reentry has taken control of the beat. Additionally, in the second image, you can see a section of the atrium that has been ablated; here, no electrical activity can occur (Video 11).

Discussion

We have demonstrated that a strand of cardiac muscles can be simulated using N-body techniques to generate a beat. This simulated strand of cardiac muscles can then be utilized to create a semi-closed mesh of cardiac tissue resembling the LA, capable of generating a beat. Muscle attributes can be introduced into the LA mesh to establish a substrate that will spontaneously develop an arrhythmia or exhibit an arrhythmia when prompted by a properly placed ectopic event. Subsequently, these arrhythmias can be rectified through simulated ablations. Because the model is interactive and can exhibit characteristics of many known LA arrhythmias, we believe this model could be a valuable tool for electrophysiologists, researchers, and medical students seeking a deeper understanding of LA arrhythmias and strategies for their elimination.

If spatial and electrical data could be extracted from a patient and incorporated into the model, it could reveal insights about that specific patient's condition. Electrophysiologists could then utilize the model to test ablation scenarios outside of the operating room.

We have successfully set up conditions in the model that induce the LA to exhibit an arrhythmia resembling AF. However, these current conditions seem somewhat contrived and lack realism. To improve the model's authenticity, we are adding thickness to move beyond a simple mesh representing the shape of the LA. Additionally, stochastic elements are being introduced to the model, incorporating small random fluctuations in muscle actions. Furthermore, we are exploring the integration of chemical waves into the model, influencing muscle properties as they pass through. We also plan to replace the central pushback force that simulates blood pressure with simulated blood.

Hardware and software

The main body of the code is written in C and C++. The computationally intensive portions were implemented in Compute Unified Device Architecture (CUDA) and offloaded to the Graphics Processing Units (GPUs) for acceleration [48,49]. The nodes and muscles of the underlying LA structure were generated in Blender using a Python API. These nodes and muscles were then stored in an input file, which was

read into our program for constructing the atrium's structure. NVIDIA Nsight was used for code optimization, and the graphical interface was developed using the Open Graphics Library (OpenGL) [50,51].

N-body simulations can be optimized to run efficiently on parallel hardware, such as NVIDIA GPUs. The software was developed and tested on a workstation equipped with two RTX A6000 GPUs, each with over 10,000 CUDA cores and 48 GB of GDDR6 video memory. The software was demonstrated to medical professionals on a laptop equipped with a single NVIDIA GTX 3080 GPU. It is worth noting that the code is relatively lightweight and does not demand extremely expensive hardware for running interactive simulations.

Limitations and future work

The user can introduce areas of heterogeneity into the model through user inputs. However, many aspects of the current model are very homogeneous. Microheterogeneity can lead to a slowing of electrical conduction through areas of the tissue and is believed to be an underlying mechanism leading to arrhythmias [52,53]. The random branching structure of heart tissue, the propagation of chemical and electrical processes in neighboring regions, and the irregular tissue patterns of the LA all contribute to microheterogeneity and should be addressed to improve the model.

Heterogeneities create a non-linear framework for the electrical current in the LA to propagate through. AF, the most prominent and least understood arrhythmia, is believed to be chaotic. Chaos can only exist in a non-linear environment in three or more dimensions [54]. Hence, improving the model to study AF is a significant impetus for future work.

Additionally, Bachmann's Bundle is currently simulated as a single pulse node that periodically attempts to initiate LA contraction. In reality, Bachmann's Bundle is a branching network of specialized myocytes that extend into the LA. This limitation also needs to be addressed to add realism to the model.

The model in its current state can be used to study periodic arrhythmias but lacks the complexity necessary to study the chaotic nature of AF. We are actively working on addressing these limitations, in addition to the enhancements described in the discussion section. Upon completion of these tasks, we will use the model to gain insights into the underlying mechanisms that cause AF.

Conclusion

The study has shown that N-body techniques can be used to construct an interactive model of the left atrium. Users can set up conditions in a live simulation that will induce common arrhythmias. These arrhythmias can be observed and studied in the model and then eliminated with simulated ablations. We hope that the model can serve as a training and study tool for electrophysiologists, researchers, and medical students.

High resolution copies of Videos 1–11 can be found on YouTube at:
Media Video 1: https://youtu.be/1LfkSLHCras
Media Video 2: https://youtu.be/uiBhadBPQuk
Media Video 3: https://youtu.be/PxOR28jeF50
Media Video 4: https://youtu.be/mIRA23GSZKs
Media Video 5: https://youtu.be/9KuRWVdBDR0
Media Video 6: https://youtu.be/SaPKsIT6DkM
Media Video 7: https://youtu.be/9QzJhKyeVGc
Media Video 8: https://youtu.be/qZ7-WLGbyLQ
Media Video 9: https://youtu.be/E1mbqbofrDo
Media Video 10: https://youtu.be/xiNUzwC2G3w
Media Video 11: https://youtu.be/G_ZcHeLRRjc

Supplementary data to this article can be found online at https://doi.org/10.1016/j.jelectrocard.2024.153762.

Funding

This research was supported by the NVIDIA corporation's Applied Research Accelerator Program. Student support was provided by Tarleton State University's Presidential Excellence in Research Scholars and the Bill and Winnie Wyatt Foundation.

Author statement

We confirm that this manuscript has not been published elsewhere and is not under consideration in whole or in part by another journal. All authors have approved the manuscript and agree with submission to the Journal of Electrocardiology. The authors have no conflicts of interest to declare.

CRediT authorship contribution statement

Bryant Wyatt: Conceptualization, Supervision, Methodology. **Gavin McIntosh:** Software. **Avery Campbell:** Investigation. **Melanie Little:** Data curation. **Leah Rogers:** Writing – review & editing. **Brandon Wyatt:** Validation.

Declaration of Generative AI and AI-assisted technologies in the writing process

During the preparation of this work the authors used ChatGPT3.5 to check for spelling and other grammatical mistakes. After using this tool, the authors reviewed and edited the content as needed and take full responsibility for the content of the publication.

Declaration of competing interest

The authors declare that there is no conflict of interest.

Data availability

The code used in this work is available on GitHub at: https://github.com/TSUParticleModelingGroup/LeftAtrium-Model.

Acknowledgments

We would like to thank Tarleton State University's Mathematics Department for use of their High-Performance Computing lab for the duration of this project. We would also like to thank Derek Hopkins for his work on the GitHub repository for this article and Hayden Rawlings for his insight into John Conway's Game of Life.

References

[1] World Health Organization. The top 10 causes of death. World Health Organization; 12/9/2020. https://www.who.int/news-room/fact-sheets/detail/the-top-10-causes-of-death.
[2] Virani SS, Alonso A, Aparicio HJ, Benjamin EJ, Bittencourt MS, Callaway CW, et al. Heart disease and stroke statistics-2021 update: a report from the American Heart Association. Circulation 2021 Feb 23;143(8):e254–743. https://doi.org/10.1161/CIR.0000000000000950. Epub 2021 Jan 27. PMID: 33501848.
[3] Brundel BJJM, Ai X, Hills MT, Kuipers MF, Lip GYH, de Groot NMS. Atrial fibrillation. Nat Rev Dis Primers 2022;8(1):21.
[4] Staerk L, Sherer JA, Ko D, Benjamin EJ, Helm RH. Atrial fibrillation. Circ Res 2017;120(9):1501–17.
[5] Pellman J, Sheikh F. Atrial fibrillation: mechanisms, therapeutics, and future directions. Compr Physiol 2015;5(2):649–65.
[6] Beigel R, Wunderlich NC, Ho SY, Arsanjani R, Siegel RJ. The left atrial appendage: anatomy, function, and noninvasive evaluation. JACC Cardiovasc Imaging 2014 Dec;7(12):1251–65. https://doi.org/10.1016/j.jcmg.2014.08.009 [PMID: 25496544].
[7] Singleton MJ, Imtiaz-Ahmad M, Kamel H, O'Neal WT, Judd SE, Howard VJ, et al. Association of atrial fibrillation without cardiovascular comorbidities and stroke risk: from the REGARDS study. J Am Heart Assoc 2020 Jun 16;9(12):e016380. https://doi.org/10.1161/JAHA.120.016380 [Epub 2020 Jun 4. PMID: 32495723; PMCID: PMC7429041].

[8] Gupta S, Figueredo VM. Tachycardia mediated cardiomyopathy: pathophysiology, mechanisms, clinical features and management. Int J Cardiol 2014 Mar 1;172(1): 40–6. https://doi.org/10.1016/j.ijcard.2013.12.180. Epub 2014 Jan 8. PMID: 24447747.

[9] Antzelevitch C, Burashnikov A. Overview of basic mechanisms of cardiac arrhythmia. 2011.

[10] Long MT, Ko D, Arnold LM, Trinquart L, Sherer JA, Keppel SS, et al. Gastrointestinal and liver diseases and atrial fibrillation: a review of the literature. Therap Adv Gastroenterol 2019 Apr 2;12. https://doi.org/10.1177/1756284819832237. 1756284819832237. PMID: 30984290; PMCID: PMC6448121.

[11] Carlo P, Giuseppe A, Simone S, Filippo G, Gabriele V, Simone G, et al. A randomized trial of circumferential pulmonary vein ablation versus antiarrhythmic drug therapy in paroxysmal atrial fibrillation. J Am Coll Cardiol 2006;48(11):2340–7.

[12] Charitakis E, Metelli S, Karlsson LO, Antoniadis AP, Rizas KD, Liuba I, et al. Comparing efficacy and safety in catheter ablation strategies for atrial fibrillation: a network meta-analysis. BMC Med 2022;20(1):193.

[13] Cheng E, Liu C, Yeo I, Markowitz S, George T, Ip J, et al. Risk of mortality following catheter ablation of atrial fibrillation. J Am Coll Cardiol 2019;74(18):2254–64.

[14] Mujović N, Marinković M, Lenarczyk R, Tilz R, Potpara TS. Catheter ablation of atrial fibrillation: an overview for clinicians. Adv Ther 2017;34(8):1897–917.

[15] Cappato R, Calkins H, Chen S-A, Davies W, Iesaka Y, Kalman J, et al. Updated worldwide survey on the methods, efficacy, and safety of catheter ablation for human atrial fibrillation. Circ Arrhythm Electrophysiol 2010;3(1):32–8.

[16] Ganesan AN, Shipp NJ, Brooks AG, Kuklik P, Lau DH, Lim HS, et al. Long-term outcomes of catheter ablation of atrial fibrillation: a systematic review and meta-analysis. J Am Heart Assoc 2013;2(2).

[17] Quah JX, Dharmaprani D, Lahiri A, Tiver K, Ganesan AN. Reconceptualising atrial fibrillation using renewal theory: a novel approach to the assessment of atrial fibrillation dynamics. Arrhythmia Electrophysiol Rev 2021;10(2):77–84. 2021.

[18] Markides V, Schilling RJ. Atrial fibrillation: classification, pathophysiology, mechanisms and drug treatment. Heart 2003 Aug;89(8):939–43. https://doi.org/10.1136/heart.89.8.939. PMID: 12860883; PMCID: PMC1767799.

[19] Wyndham CRC. Atrial fibrillation: the most common arrhythmia. Tex Heart Inst J 2000;27(3):257–67.

[20] Cheniti G, Vlachos K, Pambrun T, Hooks D, Frontera A, Takigawa M, et al. Atrial fibrillation mechanisms and implications for catheter ablation. Front Physiol 2018; 9.

[21] Gussak G, Pfenniger A, Wren L, Gilani M, Zhang W, Yoo S, et al. Region-specific parasympathetic nerve remodeling in the left atrium contributes to creation of a vulnerable substrate for atrial fibrillation. JCI Insight 2019 Oct 17;4(20):e130532. https://doi.org/10.1172/jci.insight.130532. PMID: 31503549; PMCID: PMC6824299.

[22] Potse M. Scalable and accurate ECG simulation for reaction-diffusion models of the human heart. Front Physiol 2018 Apr 20;(9):370. https://doi.org/10.3389/fphys.2018.00370. PMID: 29731720; PMCID: PMC5920200.

[23] Sellami H, Cazenille L, Fujii T, Hagiya M, Aubert-Kato N, Genot AJ. Accelerating the finite-element method for reaction-diffusion simulations on GPUs with CUDA. Micromachines (Basel) 2020 Sep 22;11(9):881. https://doi.org/10.3390/mi11090881. PMID: 32971889; PMCID: PMC7569852.

[24] Trayanova NA. Whole-heart modeling: applications to cardiac electrophysiology and electromechanics. Circ Res 2011;108(1):113–28.

[25] Espinosa Cristian Barrios, Sanchez Jorge, Dossel Olaf, Loewe Axel. Diffusion reaction eikonal alternant model: towards fast simulations of complex cardiac arrhythmias. Comput Cardiol 2022;49.

[26] Gokhale TA, Medvescek E, Henriquez CS. Modeling dynamics in diseased cardiac tissue: impact of model choice. Chaos 2017 Sep;27(9):093909. https://doi.org/10.1063/1.4999605. PMID: 28964161; PMCID: PMC5568867.

[27] Makowiec D, Wdowczyk J, Struzik ZR. Heart rhythm insights into structural remodeling in atrial tissue: timed automata approach. Front Physiol 2019 Jan 14;9: 1859. https://doi.org/10.3389/fphys.2018.01859. PMID: 30692928; PMCID: PMC6340163.

[28] Cox BN, Snead ML. Cells as strain-cued automata. J Mech Phys Solids 2016 Feb;87: 177–226. https://doi.org/10.1016/j.jmps.2015.11.002. Epub 2015 Dec 2. PMID: 31178602; PMCID: PMC6550492.

[29] Fournier Billy J, Wyatt Bryant M. Matter and GPUs: should the focus of our modeling classes be adjusted?. In: International conference on technology in collegiate mathematics. Boston, Ma: Pearson Publishing; 2016.

[30] Kim JM, Bursac N, Henriquez CS. A computer model of engineered cardiac monolayers. Biophys J 2010 May 19;98(9):1762–71. https://doi.org/10.1016/j.bpj.2010.01.008. PMID: 20441739; PMCID: PMC2862160.

[31] Tveito A, Jæger KH, Kuchta M, Mardal KA, Rognes ME. A cell-based framework for numerical modeling of electrical conduction in cardiac tissue. Front Phys 2017 Oct 10;5:48.

[32] Gerhardt M, Schuster H, Tyson JJ. A cellular automation model of excitable media including curvature and dispersion. Science 1990 Mar 30;247(4950):1563–6. https://doi.org/10.1126/science.2321017 [PMID: 2321017].

[33] Conway JH. The game of life. Sci Am 1970;223(4):4–23.

[34] Helbing D. Agent-based modeling. In: Helbing D, editor. Social self-organization. Understanding complex systems. Berlin, Heidelberg: Springer; 2012. https://doi.org/10.1007/978-3-642-24004-1_2.

[35] Sego TJ, Sluka James P, Sauro Herbert M, Glazier James A. Tissue forge: interactive biological and biophysics simulation environment. PLoS Comput Biol October 23, 2023. https://doi.org/10.1371/journal.pcbi.1010768.

[36] Greenspan D. N-body problems and models. World Scientific; 2004.

[37] Greenspan D. Molecular and particle modeling of laminar and turbulent flows. World Scientific; 2005.

[38] Wyatt Bryant M, Petz Jonathan M, Sumpter William J, Turner Ty R, Smith Edward L, Fain Baylor G, et al. Creating an isotopically similar earth-moon system with correct angular momentum from a giant impact. J Astrophys Astr 2018;39(2):1–6. 26.

[39] Eiland Justin C, Salzillo Travis C, Hokr Brett H, Highland Justin L, Mayfield William D, Wyatt Bryant M. Lunar-forming giant impact model utilizing modern graphics processing units. J Astrophys Astr 2014;35(4):607–18.

[40] Greenspan D. Quasimolecular modelling. World Scientific; 1991.

[41] Wyatt Bryant M. Collisions of microdrops of water. Comput Math Appl 1994;28 (10–12):175–208.

[42] Domine Jaryd, Grant Hakiem, Young Wyatt, Vuddandam Rajesh, Wyatt Bryant. N-body adaptive optimization of lattice towers. In: GPU Technology Conference. San Jose, CA; 2020. https://www.nvidia.com/content/dam/en-zz/Solutions/gtc/conference-posters/gtc2020-posters/Design_Engineering_01_P21881_Jaryd_Domine_Web.pdf.

[43] Greenspan D. Arithmetic applied mathematics. Pergamon Press; 1980.

[44] Greenspan D. Numerical solution of ordinary differential equations for classical, relativistic and nano systems. WILEY-VCH Verlag GmbH & Co. KGaA; 2006.

[45] Angel Edward. OpenGL: a primer. Addison-Wesley; 2002.

[46] Iwasaki Yu-ki, Nishida Kunihiro, Kato Takeshi, Nattel Stanley. Atrial fibrillation pathophysiology. Circulation 2011;124(20):2264–74.

[47] Printables. Left atrium of the heart: print for occluder implantation feasibility. https://www.printables.com/model/16719-left-atrium-of-the-heart-print-for-occluder-implan; 2020.

[48] Farber R. CUDA application design and development. In: CUDA application design and development; 2011.

[49] Jason Sands J, Kandrot E. CUDA by example: an introduction to general-purpose GPU programming. Pearson Education, Inc.; 2010.

[50] Hwu W. In: Emerald, editor. GPU computing gems. Boston, MA: Elsevier Inc.; 2011.

[51] Sellers GWRHN. OpenGL SuperBible. Boston, MA: Addison Wesley; 2014.

[52] Kucera JP, Kléber AG, Rohr S. Slow conduction in cardiac tissue, II: effects of branching tissue geometry. Circ Res 1998 Oct 19;83(8):795–805. https://doi.org/10.1161/01.res.83.8.795 [PMID: 9776726].

[53] Gokhale TA, Asfour H, Verma S, Bursac N, Henriquez CS. Microheterogeneity-induced conduction slowing and wavefront collisions govern macroscopic conduction behavior: a computational and experimental study. PLoS Comput Biol 2018 Jul 16;14(7):e1006276. https://doi.org/10.1371/journal.pcbi.1006276. PMID: 30011279; PMCID: PMC6062105.

[54] Strogatz SH. Nonlinear dynamics and chaos: with applications to physics, biology, chemistry, and engineering. CRC Press; 2018.